

# Unmodified Fe<sub>3</sub>O<sub>4</sub> nanostructure promoted with external magnetic field: safe, magnetically recoverable, and efficient nanocatalyst for N- and C-alkylation reactions in green conditions

Ezzat Rafiee<sup>1,2</sup> · Mohammad Joshaghani<sup>1,2</sup> · Parvaneh Ghaderi-Shekhi Abadi<sup>2</sup>

Received: 13 July 2017 / Accepted: 18 December 2017  
© Springer Science+Business Media B.V., part of Springer Nature 2017

**Abstract** Transition metal compounds have emerged as suitable catalysts for organic reactions. Magnetic compounds as soft Lewis acids can be used as catalysts for organic reactions. In this report, the Fe<sub>3</sub>O<sub>4</sub> nanostructures were obtained from Fe<sup>2+</sup> and Fe<sup>3+</sup>-salts, under an external magnetic field (EMF) without any protective agent. The X-ray photoelectron spectroscopy, scanning electron microscopy, and energy dispersive X-ray spectroscopy tools were used to characterize these magnetic compounds. The two-dimensional (2-D, it showed nanometric size in the two dimensions, nanorod structure) Fe<sub>3</sub>O<sub>4</sub> compound showed high catalytic activity and stability in N- and C-alkylation reactions. A diverse range of N- and C-alkylation products were obtained in moderate to high yield under green and mild conditions in air. Also the N- and C-alkylation products can be obtained with different selectivity and yield by exposure reactions with EMF. Results of alkylation reactions showed that the presence of Fe(II) and Fe(III) species on the surface of magnetic catalysts (phase structure of magnetic compounds) are essential as very cheap active sites. Also, morphology of magnetic catalysts had influence on their catalytic performances. After the reaction, the catalyst/product(s) separation could be easily achieved with an external magnet and more than 95% of catalyst could be recovered. The catalyst was reused at least four times without any loss of its high catalytic activity for N- and C-alkylation reactions.

**Keywords** Fe<sub>3</sub>O<sub>4</sub> · External magnetic field · Two-dimensional array · Magnetic nanostructure catalyst

---

✉ Ezzat Rafiee  
ezzatz\_rafiee@yahoo.com; e.rafiei@razi.ac.ir

<sup>1</sup> Department of Inorganic Chemistry, Faculty of Chemistry, Razi University, Tagh-e-Bostan, PO Box 67346-67149, Kermanshah 67149, Iran

<sup>2</sup> Institute of Nanoscience and Nanotechnology, Razi University, Tagh-e-Bostan, PO Box 67346-67149, Kermanshah 67149, Iran

## Introduction

Due to the low cost of Fe compounds compared to Au, Ag, Pd, Pt, Ru, and Rh compounds, it has attracted particular attention as a catalyst for various organic reactions [1]. The first example of using unprotected magnetite compounds as catalyst was reported in the four-component Aza-Sakuray reaction [2–7]. Then these catalysts were applied in N-alkylation reactions [8], trisubstituted imidazoles synthesis [9], and Sonogashira–Hagihara reactions [10]. These compounds, due to nontoxicological features, ease and various preparation processes, being commercially accessible, and not time-consuming separation of them from reaction mixtures, have attracted widespread attention as catalyst in the past decades [11, 12]. These properties are a subject of interest for investigation, especially for large-scale operation in industries.

Among the different magnetic compounds,  $\text{Fe}_3\text{O}_4$  are used as a catalyst in carbon–carbon double bond isomerization [13], modified Fischer–Tropsch reactions [14], water–gas shift reactions [15], dehydrogenation [16], and epoxidation [17] reactions. Catalytic activity of  $\text{Fe}_3\text{O}_4$  in these reactions is due to various parameters, for example, a surface of  $\text{Fe}_3\text{O}_4$  (111) terminated by a hexagonal oxygen layer covered by one quarter monolayer of iron cations, these Lewis acid centres act as active centers [18].

Many efficient techniques were developed for preparing micro- and nano-size  $\text{Fe}_3\text{O}_4$  [19]. Recent developments have indicated that the magnetic field, in an elegant way, could be applied for preparation and orientation of magnetic compounds into nano- or microscale structures [9, 20, 21]. For magnetic compounds, an external magnetic field (EMF) can be manipulated for spin, charge, and orbital degrees of freedom that lead to rearrangements of electrons and magnetic domains in atomic and molecular systems [22]. Therefore, these changes affect physical and chemical reactivity of magnetic compounds [23, 24].

Also, an especially interesting topic is whether such organic reactions may be controlled by an EMF. A few experimental observations have been reported which illustrate the possibility of utilizing EMF in the field of heterogeneous catalysis. In an early review from 1975, studies of CuO nanoparticles revealed that a weak magnetic field can cause a change from antiferromagnetic to ferromagnetic spin ordering and increase ammonia adsorption [25, 26]. In the presence of a weak magnetic field, CO oxidation on nonmagnetic Pt catalyst supported on carbon coated magnetic Co particles has been investigated [27]. Also, the activation energy for NO reduction was found to be reduced under a magnetic field, leading to an increase in conversion rate [28].

According to the above studies, our group decided to apply EMF in the synthesis of  $\text{Fe}_3\text{O}_4$  and use this catalyst as a typical heterogeneous Lewis acid in N- and C-alkylation reactions. Alkylation reactions during green and mild conditions [29, 30], base-free systems [29], and by non-noble metal catalyst [29, 30] with only  $\text{H}_2\text{O}$  as byproduct have attracted much attention by our group. Also, to investigate the effect of EMF on alkylation reaction, the N- and C-alkylation reactions were carried out under exposure of EMF in the presence of the magnetic catalyst.

## Experimental

### Materials

FeCl<sub>3</sub>·6H<sub>2</sub>O, FeCl<sub>2</sub>·4H<sub>2</sub>O, commercial Fe<sub>3</sub>O<sub>4</sub>, NaOH, aromatic compounds, amines, alcohols, solvents, and bases were purchased from Merck, Germany, with analytical grades and these were used without further purification.

### Preparation of magnetic nanostructure catalysts

In a typical procedure [9], FeCl<sub>3</sub>·6H<sub>2</sub>O (0.06 mol) and FeCl<sub>2</sub>·4H<sub>2</sub>O (0.03 mol) were dissolved into 5.0 ml of deoxygenated water (by nitrogen gas bubbling). The resulting solution was added dropwise into 25 ml NaOH (1.5 M) under vigorous mechanical stirring at room temperature. The overall experimental process was directly performed in a Helmholtz cylinder permanent magnet with a value of 362–526 μT. A black precipitate formed after 20 min. After synthesis treatment, the resulting black precipitate was collected, filtered, and washed with deoxygenated distilled water several times to remove any possible impurities, and finally dried in a desiccator at room temperature before characterization. The as-obtained crystalline Fe<sub>3</sub>O<sub>4</sub> sample was denoted as the **AEMF1–AEMF6** (applied external magnetic field 362–526, respectively) catalyst (Table 1).

For synthesis of **AEMF4**, a mixture of iron salts in deoxygenated water and NaOH solution was exposed to EMF (362 μT) for 5 min. Then EMF was removed and the mixture was stirred for 15 min under vigorous mechanical stirring.

**Table 1** Experimental conditions for preparation of different magnetic catalysts with various abbreviations

No.	Intensity of EMF (μT)	Phase structure <sup>a</sup>	Average crystallite size (nm) <sup>b</sup>	Morphologies of the products <sup>c</sup>	Symbol
1	0	Fe <sub>3</sub> O <sub>4</sub> /Fe <sub>2</sub> O <sub>3</sub>	34.03	Peg-like	<b>ZEMF</b> (Zero external magnetic field)
2	362	Fe <sub>3</sub> O <sub>4</sub> /FeO	23.10	Rod-like	<b>AEMF1</b>
3	432	Fe <sub>3</sub> O <sub>4</sub>	23.69	Amorphous	<b>AEMF2</b>
4	485	Fe <sub>3</sub> O <sub>4</sub>	23.57	Amorphous	<b>AEMF3</b>
5	362	Fe <sub>3</sub> O <sub>4</sub>	22.22	Rod-like	<b>AEMF4</b>
6	362	Fe <sub>3</sub> O <sub>4</sub>	20.98	Rod-like	<b>AEMF5</b>
7	362	Fe <sub>3</sub> O <sub>4</sub> /FeO	17.20	Sheet-like	<b>AEMF6</b>

Reaction conditions: FeCl<sub>3</sub>·6H<sub>2</sub>O (0.06 mol), FeCl<sub>2</sub>·4H<sub>2</sub>O (0.03 mol), deoxygenated water (5.0 ml), NaOH (1.5 M), time = 20 min

<sup>a</sup>According to XRD patterns and FT-IR results reported previously by our group [9]

<sup>b</sup>According to XRD patterns results reported previously by our group [9]

<sup>c</sup>According to scanning electron microscopy (SEM) results reported previously by our group [9]

For synthesis of **AEMF5**, a mixture of iron salts in deoxygenated water and NaOH solution was stirred for 15 min under vigorous mechanical stirring. Then the mixture was exposed to EMF (362  $\mu$ T) for 5 min.

For synthesis of **AEMF6**, a mixture of iron salts in deoxygenated water and NaOH solution was exposed to EMF (362  $\mu$ T) for 5 min. Then EMF was removed and the mixture was stirred for 5 min under vigorous mechanical stirring. This condition was repeated for two times.

## Methods

The magnetic field was generated by a Helmholtz cylinder permanent magnet, Iran, and fuel source. The bore diameter was 3 cm, and an AC magnetic flux density in the range of 362–526  $\mu$ T could be imposed. The X-ray photoelectron spectroscopy (XPS) was recorded by a Kratos Analytical Axis Ultra, Shimadzu, Japan, with monochromatic aluminum and magnesium with X-ray source of 1486.6 and 1253.6 eV and a Concentric Hemispherical Analyzer (CHA). A take-off angle of 90° was used on a spot size of 700  $\mu$ m  $\times$  350  $\mu$ m. The instrument has Ultra High Vacuum (UHV). The scanning electron microscopy (SEM) has been performed using an AIS2300C microscope, Japan, with a scanning range from 0 to 20 keV. The energy dispersive X-ray (EDX) measurement was made with an IXRF model 550i, Japan, attached to SEM. SEM/EDX samples were prepared by coating of solid particles into a conductive layer.

## General procedure for the N-alkylation reaction

In a typical reaction, a suspension of amine (1.0 mmol) and alcohol (1.0 mmol) was added to a mixture of magnetic catalyst (0.04 g) with 1.5 ml distilled water. The resulting mixture was heated to 40 °C for an appropriate time under aerobic conditions. In the case of exposure by EMF, the resulting mixture was transferred to a Helmholtz cylinder permanent magnet and exposed with 362  $\mu$ T intensity for an appropriate time. Progress of the reaction was monitored by TLC. After completion of the reaction, the mixture was cooled to room temperature, and the catalyst was separated from the product solution using an external magnet, washed with deoxygenated distilled water, dried in a desiccator at room temperature, and used for the next reaction cycle without any pre-treatment. Solvent of the reaction mixture was evaporated to generate the crude product. The product was concentrated and purified by column chromatography on silica-gel using EtOAc/heptane (1:4) as eluent.

## General procedure for the C-alkylation reaction

In a typical reaction, a suspension of the magnetic catalyst (0.004 g), alcohol (1.0 mmol), and aromatic compound (2.5 ml) were mixed in a reaction flask. The reaction mixture was stirred at 60 °C for an appropriate amount of time. In the case of exposure by EMF, the resulting mixture was transferred to a Helmholtz cylinder permanent magnet and exposed with 432  $\mu$ T intensity for an appropriate time.

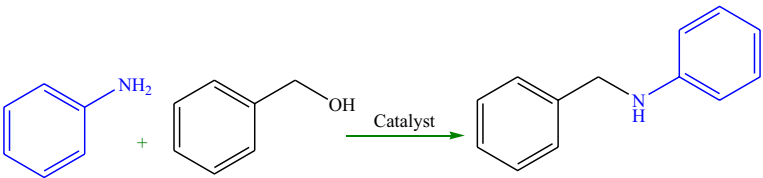
Progress of the reaction was monitored by TLC. After the complete conversion, the reaction mixture was allowed to cool to room temperature. The catalyst was separated from the product solution using an external magnet, washed with deoxygenated distilled water, dried in a desiccator at room temperature and used for the next reaction cycle without any pretreatment. Solvent of the reaction mixture was evaporated to generate the crude product. The product was concentrated and purified by column chromatography on silica-gel using EtOAc/heptane (1:3) as eluent.

## Results and discussion

### General procedure for optimization of the N-alkylation reaction conditions

We initially conducted the reaction of aniline and benzyl alcohol as a model reaction. A series of parameters were optimized in this reaction (Table 2).

With 0.02 g **AEMF1**, four different temperatures were evaluated in the model reaction (Table 2, entries 1–4). Increase of the temperature from 40 to 80 °C shows no significant effect on the yield of the corresponding product. Besides, N-alkylation reaction was uncompleted at room temperature. Then other reactions were performed at 40 °C. The use of 0.04 g of the catalyst increased the reaction yield up to 85% after 20 min (Table 2, entries 2 and 5). Besides, in the absence of the catalyst, the reaction exhibited very low yield although in a longer reaction time (Table 2, entry 6). The base employed in the reaction also seems to be important, in the presence of NaOH, low yield of corresponding product was obtained (Table 2, entry 7). However, the relevant yield was obtained when the alkylation reaction was carried out in base-free conditions (Table 2, entry 8). Interestingly, similar results were obtained in polar or nonpolar solvents (Table 2, entries 8, 9), which implies there are no relevant solvent polarity effects under these conditions. When the reaction was carried out in solvent-free condition, low yield was obtained at a high reaction time (Table 2, entry 10). Equimolar amounts of aniline and benzyl alcohol (1.0 mmol) resulted in excellent yield of the product compared with other ratios (Table 2, entries 8, 11, 12). We tested the catalytic efficacy of other magnetic catalysts in the N-alkylation reaction with optimized reaction conditions (Table 2, entries 13–19). It seems that **AEMF1** and **AEMF6** as catalysts showed the best performance (Table 2, entries 11, 17). Because the synthetic procedure of the **AEMF6** is tedious and not technically simple [15], **AEMF1** was chosen as the best catalyst (Table 2, entry 11). According to the above results, the phase structure of magnetic nanocompounds (Table 1) greatly influences their catalytic performance. The alkylation reaction using ZEMF due to presence Fe<sub>2</sub>O<sub>3</sub> (Table 1, entry 1), which presents distribution Fe(III) on a surface, is not suitable (Table 2, entry 18). However, the alkylation reaction using Fe<sub>3</sub>O<sub>4</sub> and FeO in magnetic catalysts (**AEMF1**–**AEMF6**, Table 1, entries 2–7), which have their surface layer terminated purely by oxygen atoms, gave a significant result (Table 2, entries 11, 13–17) [7, 31]. These results pointed out that the reaction seemed to be more catalysed by Fe(II) compared to Fe(III) centres [32, 33]. Also, the morphology of magnetic nanocatalysts [9] may be influenced by their catalytic performance due to the difference in adsorption/desorption of reaction

**Table 2** Optimization of the N-alkylation reaction conditions


Entry	PhNH <sub>2</sub> :PhCH <sub>2</sub> OH (molar ratio)	Catalyst (g)	Temp. (°C)	Solvent	Base	Time (min)	Yield (%) <sup>a</sup>
1	1:2	<b>AEMF1</b> /(0.02)	r.t.	Water	NaO <sup>t</sup> Bu	20 (2 h)	0 (51)
2	1:2	<b>AEMF1</b> /(0.02)	40	Water	NaO <sup>t</sup> Bu	20	70
3	1:2	<b>AEMF1</b> /(0.02)	60	Water	NaO <sup>t</sup> Bu	20	78
4	1:2	<b>AEMF1</b> /(0.02)	80	Water	NaO <sup>t</sup> Bu	20	80
5	1:2	<b>AEMF1</b> /(0.04)	40	Water	NaO <sup>t</sup> Bu	20	85
6	1:2	–	40	Water	NaO <sup>t</sup> Bu	20 (60)	0 (19)
7	1:2	<b>AEMF1</b> /(0.04)	40	Water	NaOH	20 (50)	19 (59)
8	1:2	<b>AEMF1</b> /(0.04)	40	Water	–	20 (30)	71 (93)
9	1:2	<b>AEMF1</b> /(0.04)	40	Toluene	–	20	90
10	1:2	<b>AEMF1</b> /(0.04)	40	–	–	20 (60)	10 (51)
11	1:1	<b>AEMF1</b> /(0.04)	40	Water	–	20 (30)	40 (96)
12	2:1	<b>AEMF1</b> /(0.04)	40	Water	–	20 (2 h)	0 (42)
13	1:1	<b>AEMF2</b> /(0.04)	40	Water	–	20 (50)	35 (93)
14	1:1	<b>AEMF3</b> /(0.04)	40	Water	–	20 (4 h)	0 (58)
15	1:1	<b>AEMF4</b> /(0.04)	40	Water	–	20 (50)	20 (85)
16	1:1	<b>AEMF5</b> /(0.04)	40	Water	–	20 (50)	20 (67)
17	1:1	<b>AEMF6</b> /(0.04)	40	Water	–	20 (30)	50 (95)
18	1:1	<b>ZEMF</b> /(0.04)	40	Water	–	20 (60)	35 (85)

Reaction conditions: Base (1.0 mmol); 1.5 ml solvent

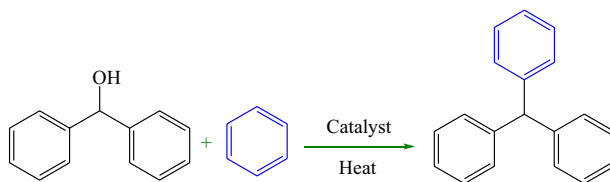
<sup>a</sup>Isolated yield

molecules, involving substrates, intermediates, and target product on different crystal facets of magnetic catalysts surfaces with the different morphologies [34–38].

### General procedure for optimization of the C-alkylation reaction conditions

Benzene and benzhydre were selected as a model substrate for the C-alkylation reaction. A series of parameters were optimized in this reaction (Table 3).

With 0.002 g **AEMF1**, three different temperatures were evaluated in the model. When the reaction was performed at 60 °C, the expected product was afforded a 92% yield after 30 min (Table 3, entries 1–3). By using 0.003 and 0.004 g of the **AEMF1** as catalyst, the product was obtained in excellent yield (Table 3, entries 4 and 5). It seems that when the amount of the catalyst increased, reaction time

**Table 3** Optimization of the C-alkylation reaction conditions

Entry	Catalyst (g)	Temp. (°C)	Catalyst type	Time (min)	Yield (%) <sup>a</sup>
1	0.002	30	<b>AEMF1</b>	50	81
2	0.002	60	<b>AEMF1</b>	30	92
3	0.002	90	<b>AEMF1</b>	25	93
4	0.003	60	<b>AEMF1</b>	20	94
5	0.004	60	<b>AEMF1</b>	10	96
6	–	60	None	10 h	–
7	0.004	60	<b>AEMF2</b>	30	68
8	0.004	60	<b>AEMF3</b>	30	40
9	0.004	60	<b>AEMF4</b>	15	91
10	0.004	60	<b>AEMF5</b>	40	89
11	0.004	60	<b>AEMF6</b>	10	90
12	0.004	60	<b>ZEMF</b>	25	50

Reaction conditions: benzhydrol, (1.0 mmol) and benzene, (2.5 mL)

<sup>a</sup>Isolated yield

gradually decreased. Therefore, 0.004 g of the **AEMF1** was selected as the best catalyst loading in further investigations (Table 3, entry 5). In the absence of the catalyst, no product was formed after 10 h (Table 3, entry 6). In the later step, different catalysts were used in the model reaction. According to the results, it seems that the best C-alkylation yield was obtained for the **AEMF1** catalyst while the **AEMF2** and **AEMF3** catalysts exhibited low activity and selectivity compare with **AEMF1** (Table 3, entries 7, 8). Besides, the **AEMF4** and **AEMF5** were evaluated as catalyst (Table 3, entries 9, 10), but the results were all inferior to the **AEMF1**. In the case of **AEMF6**, which shows 90% product yield after 10 min, the reaction is not technically simple (Table 3, entry 11) [9]. On the other hand, magnetic-free catalyst (ZEMF) exhibited low activity which indicates an inevitable role of EMF as a promoter in the activity of the catalytic sites (Table 3, entry 12) [32, 33]. According to the above results, again the nature of the catalysts has a dominating effect on the yield of the products [32, 33].

According to above results, the **AEMF1** catalyst showed the best performance in N- and C- alkylation reactions (Tables 2, 3). Therefore, the reusability, catalytic mechanism, and structural properties of **AEMF1** were investigated here.

## Reusability of the AEMF1 in the N- and C-alkylation reactions

For a heterogeneous catalyst, it is important to examine its ease of separation, recoverability, and reusability. The reusability of the **AEMF1** catalyst was investigated in the N- (Table 2, entry 11) and C-alkylation (Table 3, entry 5) reactions, and experiments were properly scaled up. After each run, the catalyst was separated from mixing reaction by using an external magnet, washed with deoxygenated distilled water, dried in a desiccator at room temperature and used for the next reaction cycle without any pre-treatment. An almost consistent activity was observed for the next four consecutive cycles (Fig. 1). We consider that loss of the catalyst during the separation process after four successive runs of N- and C-alkylation reactions were 14 and 15.5 wt%, respectively (compared with the amount of fresh catalyst used in the first run).

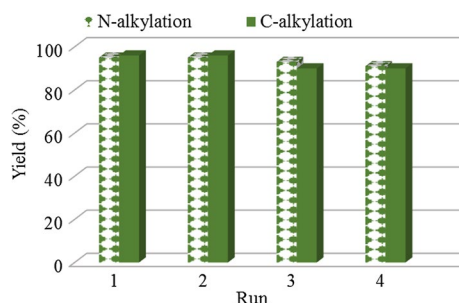
## Mechanism of the N- and C-alkylation reactions

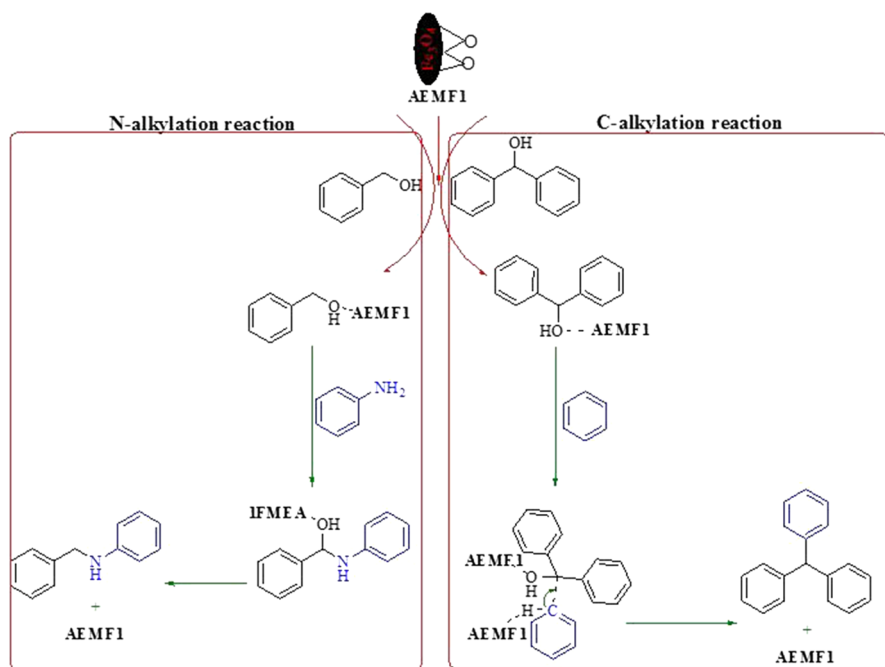
The plausible catalytic mechanism for the synthesis of corresponding N- and C-alkylation products in a model reaction in the presence of **AEMF1** is proposed in Scheme 1. According to previous results, surfaces of the magnetite  $\text{Fe}_3\text{O}_4$  and FeO are terminated by a hexagonal oxygen layer covered by a one quarter monolayer of iron cations [7, 31]. These Lewis acid centers on the surface as the active sites for chemisorption could catalyze the organic reaction [7, 9, 18]. The strong Lewis acid centers on the surface of **AEMF1** could activate the hydroxyl group in benzyl alcohol or benzhydrol [39] which was attacked by the aniline or benzene, following generation of the final N- and C-alkylation products [40].

## Characterization of the AEMF1 catalyst

The surface chemical states of the active sites in **AEMF1** were investigated using a typical high and low energy-scan XPS analysis (Fig. 2a, b). The XPS spectra indicate the presence of Fe(II) and Fe(III) octahedral species (Fig. 2b) [9, 41]. These metallic sites on the surface of **AEMF1** could activate the hydroxyl group of alcohols in N- and C-alkylation reactions. Therefore, active alcohols can be directly attacked by aniline or aromatic compounds for N- and C-alkylation reactions, respectively.

**Fig. 1** Recycling efficiency of the **AEMF1** for the N- and C-alkylation reactions





**Scheme 1** Plausible mechanism of the N- and C-alkylation reactions in the presence of the AEMF1 catalyst

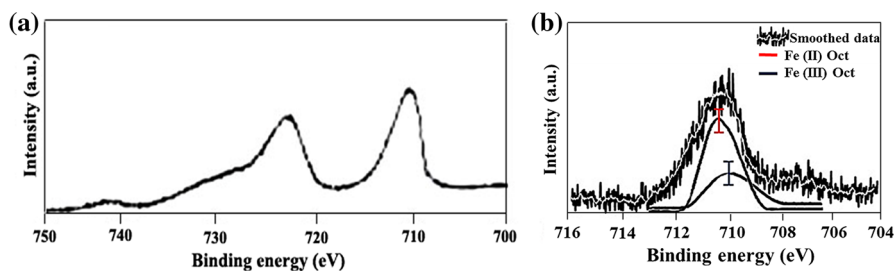


**Fig. 2** XPS analysis of AEMF1 with **a** low and **b** high resolution spectra

SEM images in Fig. 3a–c reveal that AEMF1 displays uniformly rod-like networks with an average diameter around 100–200 nm. For the crystal growth process of nanorods Fe<sub>3</sub>O<sub>4</sub> under EMF, the clusters were first grown to the aggregation nanocrystals as a bed (substrate), then the oriented nanocrystals aggregated to nanorods through Ostwald ripening on this bed along with the direction of EMF because EMF made an anisotropic media for the growth of the crystals. According to the EDX elemental mapping images for a single nanorod Fe<sub>3</sub>O<sub>4</sub> structure, Fig. 3d shows uniform distribution of Fe and O in the nanorod structure.

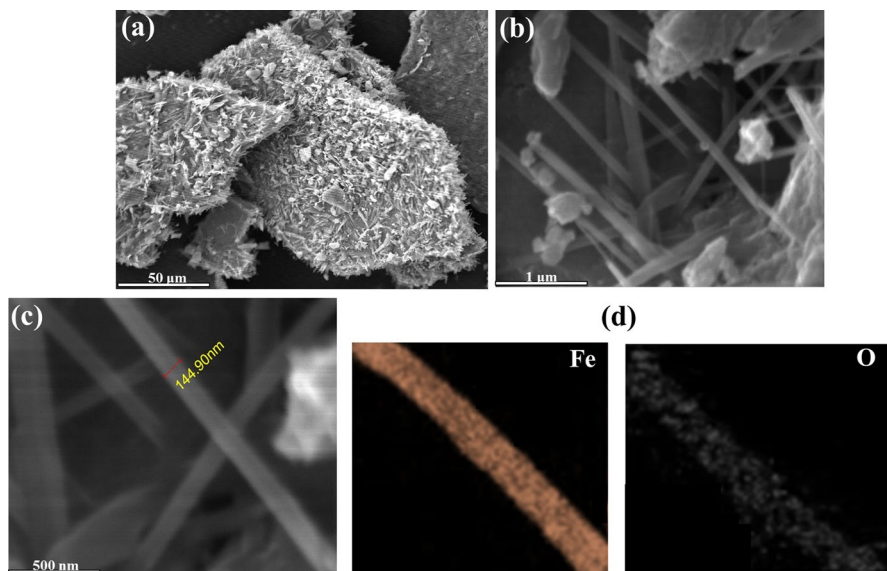


**Fig. 3** SEM images of AEMF1 in **a**, **b** low resolution, **c** high resolution, and **d** EDX elemental mapping data of a single nanorod  $\text{Fe}_3\text{O}_4$  structure

### Synthesis of various N-alkylation products

To evaluate the scope and generality of this new protocol, various amines and alcohols were tested (Table 4). We started by changing the electronic nature of the substituent on amine. Electron donating groups at the *para*-position of the arylamines afforded high yields in comparison with electron withdrawing groups at the *ortho*, *meta*, and *para*-position (Table 4, entries 2–9). It seems that formation of a hydrogen bond between the amine and nitro present on the 2-nitro-phenylamine inhibits the program of the reaction compared to 4-nitro-phenylamine (Table 4, entries 4, 6). In the case of a sterically demanding group of the arylamine, yield of the corresponding product was low at the same reaction time (Table 4, entry 10). Benzylamine was converted to its respective secondary amine in only 70% yield at a high reaction time (Table 4, entry 11); however, reaction with propan-2-amine did not occur over 12 h (Table 4, entry 12). Besides, butan-1-amine reacted within 120 min to give the desired product in 15% yield (Table 4, entry 13).

The reaction using different 4-substituted electron donating and withdrawing group alcohols with aniline gave the same results (Table 4, entries 14–17). Formation of hydrogen bond between the hydroxide and nitro group on the 2-nitrobenzyl alcohol does not show a significant effect on the yield of corresponding N-alkylation product compared to 4-nitrobenzyl alcohol (Table 4, entries 17, 18). Reaction of aniline with alkyl alcohols, occurred in high reaction times (Table 4, entries 19, 20).

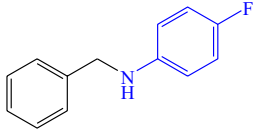
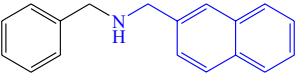
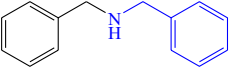
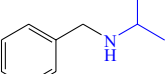
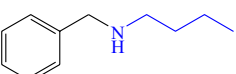
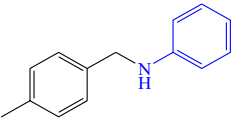
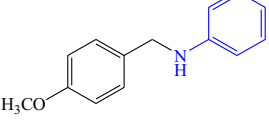
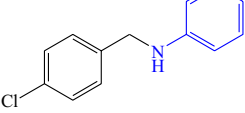
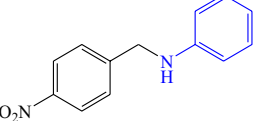
We next turned our attention to the N-alkylation reactions of heterocyclic aromatic and secondary amines with different alcohols. At first, pyridin-2-amine, pyridin-3-amine, and 4-aminopyridine with benzyl alcohol reacted efficiently to give a

**Table 4** N-alkylation of the various amines and heterocyclic aromatic amines with alcohols

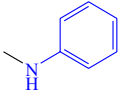
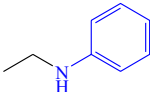
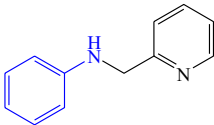
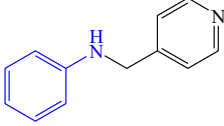
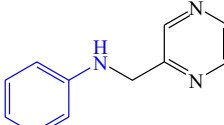
Reaction scheme: Rc1ccc(N)cc1 + R'c1ccc(CO)cc1 >> R'c1ccc(CNc2ccc(R)cc2)cc1 (Reaction conditions: AEMF1, water)

Entry	Product	Time (min)	Yield (%) <sup>a</sup>	Ref.
1		30	95	[42]
2		45	91	[43]
3		60	39	[44]
4		12 h	28	[45]
5		60	82	[45]
6		60 (2 h)	61 (74)	[45]
7		60	81	[46]

**Table 4** (continued)

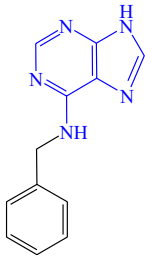
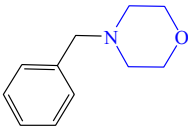
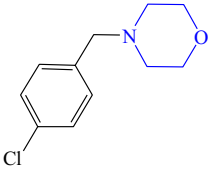
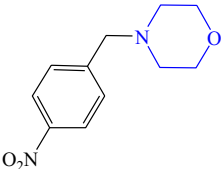
Entry	Product	Time (min)	Yield (%) <sup>a</sup>	Ref.
8		60	69	[47]
9		60 (2 h)	39 (50)	[48]
10		60 (2 h)	48 (80)	[49]
11		120 (12 h)	51 (70)	[44]
12		12 h	-	-
13		120 (12 h)	15 (30)	[46]
14		40	91	[42]
15		40	94	[42]
16		60	92	[42]
17		60	78	[42]

**Table 4** (continued)

Entry	Product	Time (min)	Yield (%) <sup>a</sup>	Ref.
18		60	70	[50]
19		3 h	60	[51]
20		3 h	58	[52]
21		3 h	70	[47]
22		3 h	71	[53]
23		3 h	82	[47]
24		12 h	-	-
25		60	95	[54]

good yield of corresponding products (Table 4, entries 21–23). The position of this extra nitrogen atom seems to have no influence on the results. An *ortho*-nitro substituted of pyridin-3-amine did not give a yield of the product even over a long reaction

**Table 4** (continued)

Entry	Product	Time (min)	Yield (%) <sup>a</sup>	Ref.
26		12 h	-	-
27		120	70	[55]
28		12 h	-	-
29		90	90	[56]

Reaction conditions: AEMF1, (0.04 g); amine and heterocyclic aromatic amines, (1.0 mmol); alcohol, (1.0 mmol); 1.5 mL water at 40 °C

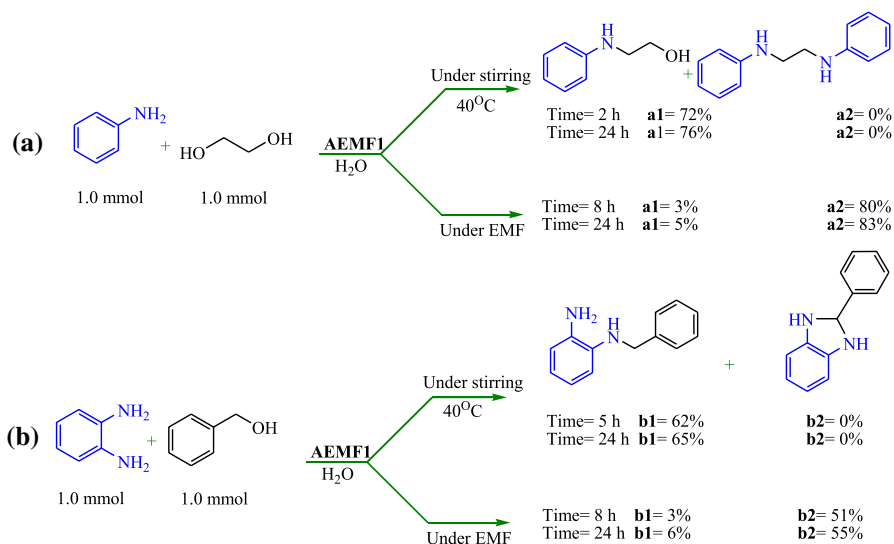
<sup>a</sup>Isolated yield; all products are identified by comparing of their spectral data with those of the authentic samples [42–56]

time, possibly due to formation of hydrogen bond between the nitro and amine group for the 3-nitropyridin-2-amine and steric reasons (Table 4, entry 24). Besides, the existence of two nitrogen atoms on the six membered ring of the amine was affected on the yield and reaction time of alkylation reaction (Table 4, entry 25). However, 9H-purin-6-amine and benzyl alcohol did not react over 12 h (Table 4, entry 26). We considered morpholine as a suitable candidate for further evaluation of the influence of AEMF1 on the N-alkylation of a cyclic secondary amine. Our catalytic system showed moderate activity for the N-alkylation of morpholine with benzyl alcohol (Table 4, entry 27). However, reaction of morpholine with 4-chlorobenzyl alcohol failed to produce the desired product (Table 4, entry 28). The alkylation reaction

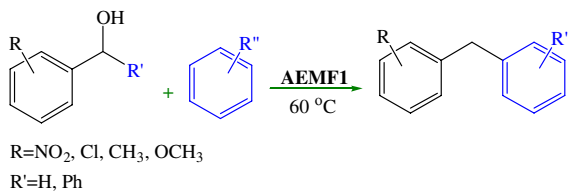
between morpholine and 4-methoxybenzyl alcohol showed high yield (Table 4, entry 29).

Ethylene glycol and benzene-1,2-diamine are interesting test substrates as amine and alcohol, because these contain double functional groups, both susceptible to the N-alkylation reaction. In the case of ethylene glycol as alcohol source, the product of first N-alkylation (Scheme 2a, **a1**) was obtained after 2 h. Products of secondary N-alkylation (Scheme 2a, **a2**) were not observed even after 24 h at 40 °C. In the case of benzene-1,2-diamine as amine source, the first N-alkylation product (Scheme 2b, **b1**) was obtained after 5 h, but the product of secondary N-alkylation (Scheme 2b, **b2**) was not observed, even after 24 h at 40 °C.

According to previous reports, yield and selectivity of the products at organic reactions are affected by exposure reaction ambience by EMF [25–28]. Therefore, we tried to increase the selectivity and yield of the diamine products in the N-alkylation reactions. Therefore, the above alkylation reactions were studied under exposure of EMF (362 μT) as modified reaction conditions. However, this reaction system offers an effective method for the synthesis of diamine products (**a2** and **b2**) with suitable yield and selectivity after 8 h (Scheme 2a and b). Under EMF, preferential and selective adsorption/desorption of reaction molecules (substrates, intermediates, and target products) on different sites of magnetic particles surface occurred [25–28].

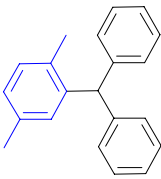
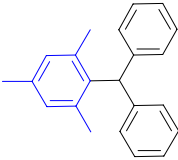
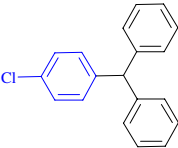
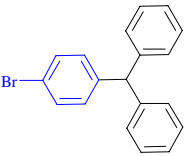


**Scheme 2** Alkylation of **a** aniline with ethylene glycol and **b** *m*-benzenediamines with benzyl alcohol using the AEMF1 catalyst in the presence and absence of EMF [57–59]

**Table 5** C-alkylation of various alcohols with aromatic compounds

Entry	Product	Time (min)	Yield (%) <sup>b</sup>	Ref. <sup>c</sup>
1		40	60	[60]
2		30	60	[61]
3		30	80	[62]
4		20	80	[61]
5		10	96	[63]
6		10	91	[64]
7		10	89	[38]

**Table 5** (continued)

Entry	Product	Time (min)	Yield (%) <sup>b</sup>	Ref. <sup>c</sup>
8		20	92	[64]
9		30	88	[64]
10		30	74	[65]
11		30	90	[65]

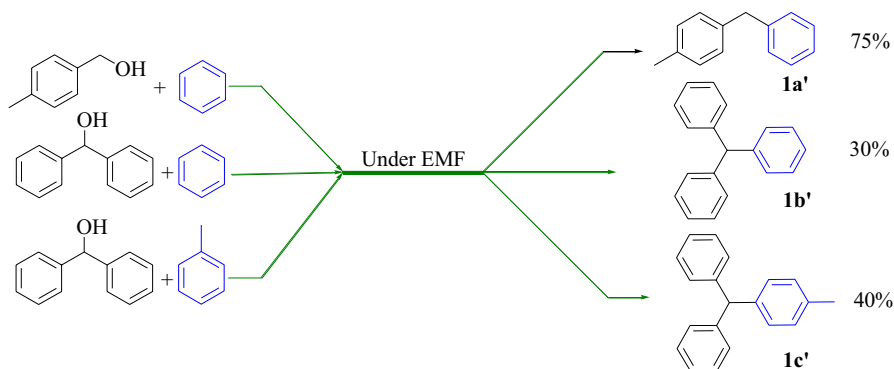
Reaction conditions: the AEMF1, (0.004 g); alcohol, (1.0 mmol); aromatic compound, (2.5 mL);  $T = 60\text{ }^{\circ}\text{C}$

<sup>a</sup>Isolated yield

<sup>b</sup>All products are known and identified by comparing of their spectral data with those of the authentic samples [38, 60–65]

### Synthesis of various C-alkylation products

To evaluate the scope and generality of this new protocol, various alcohols and aromatic compounds were employed as a substrate for the C-alkylation reaction (Table 5). Alcohols with both electron withdrawing and donating groups showed a difference in reactivity. For example, low yields were observed with electron withdrawing substituents on the benzyl alcohol (Table 5, entries 1, 2) compared with alcohols containing electron donating groups (Table 5, entries 3–5). However, according to these results, benzhydrol is a suitable selection for more investigations in C-alkylation reaction with various aromatic compounds. The C-alkylation benzhydrol with benzene, toluene, and methoxy benzene gave nearly the same and excellent yields at similar reaction times (Table 5, entries 5–7). *p*-Xylene and mesitylene obtain corresponding products in longer reaction times probably due to the steric effect (Table 5, entries 8, 9). It seems that the existence of electron



**Scheme 3** Investigation of the EMF effect on the C-alkylation reactions

withdrawing groups on the benzene reduced yield of the corresponding product and took a longer reaction time compared to the benzene as substrate (Table 5, entries 10, 11).

Toward an investigative effect of EMF on the C-alkylation reaction, some of alkylation reactions reported in Table 5 entries 3, 5, 6 were selected and carried out under EMF (432  $\mu$ T). Yield for the **1b'** and **1c'** products (Scheme 3) were decreased (compared to **1b** and **1c**, entries 5, 6 of Table 5) at 20 min of reaction time without any progress (Fig. 4). The reaction profiles of these reactions are shown in Fig. 4. According to the results, the reaction rates under EMF were higher at the start of the reaction. The EMF can lead to activation of the magnetic catalyst for the first occurrence of the reaction but, due to the agglomeration of the magnetic catalyst during reaction, its surface area decreases. These phenomena may be the basic reason for lower activity of the magnetic catalyst in the C-alkylation reaction [9, 66, 67].

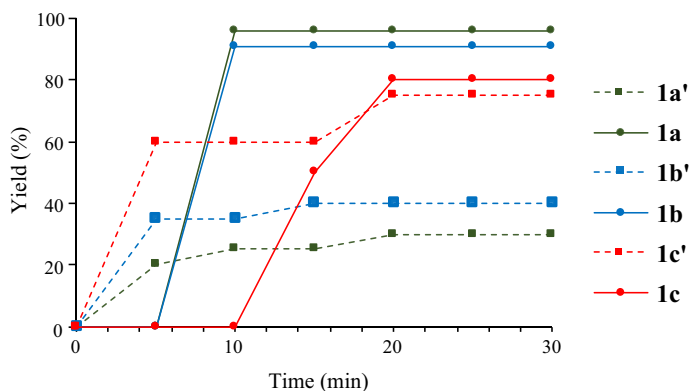


**Fig. 4** Reaction profiles of the C-alkylation of benzhydrol and benzene (**1a'**, green dash line), benzhydrol and toluene (**1b'**, blue dash line), *p*-tolyl-methanol and benzene (**1c'**, red dash line), and under exposure EMF of benzhydrol and benzene (green solid line), benzhydrol and toluene (blue solid line), *p*-tolyl-methanol and benzene (red solid line) during 30 min tracking in the presence of AEMF1 catalyst. (Color figure online)

## Conclusion

In summary, Fe<sub>3</sub>O<sub>4</sub> synthesized under EMF as a promoter and a resistor. N- and C-alkylation reactions catalyzed using a cheap, simple, and non-toxic nanorod Fe<sub>3</sub>O<sub>4</sub> catalyst. Under these conditions, alkylation reactions had high activity and selectivity under green and mild conditions. Also, alkylation reactions were carried out under EMF to investigate the EMF effect. The Fe<sub>3</sub>O<sub>4</sub> catalyst was analyzed using the XPS, SEM, and EDX analyses. It seems that a special phase structure and the morphology of Fe<sub>3</sub>O<sub>4</sub> compound have very important effects on its catalytic activity. Fe<sub>3</sub>O<sub>4</sub> catalyst with high stability was recovered and reused very easily in N- and C-alkylation reactions. The simple recyclability makes this catalyst suitable for continuous industrial processes.

**Acknowledgements** The authors thank the Razi University Research Council for support of this work.

## References

1. X. Jian, B. Wu, Y. Wei, S. Xue Dou, X. Wang, W. He, N. Mahmood, *ACS Appl. Mater Interfaces* **8**(9), 6101 (2016)
2. D.J. Kim, Y.K. Lyu, H.N. Choi, I.H. Min, W.Y. Lee, *Chem. Commun.* **23**, 2966 (2005)
3. A. Hu, G.T. Yee, W. Lin, *J. Am. Chem. Soc.* **127**, 12486 (2005)
4. A.H. Lu, E.L. Salabas, F. Sch'uth, *Angew. Chem. Int. Ed.* **46**, 1222 (2007)
5. S. Laurent, D. Forge, M. Port, A. Roch, C. Robic, L. Vande Elst, R.N. Muller, *Chem. Rev.* **108**, 2064 (2008)
6. Y. Jiang, J. Jiang, Q. Gao, M. Ruan, H. Yu, L. Qi, *Nanotechnology* **19**, 075714 (2008)
7. R. Mart'inez, D.J. Ram'on, M. Yus, *Adv. Synth. Catal.* **350**, 1235 (2008)
8. C. Gonzalez-Arellano, K. Yoshida, R. Luque, P.L. Gai, *Green Chem.* **12**, 1281 (2010)
9. E. Rafiee, M. Joshaghani, P.G.-S. Abadi, *RSC Adv.* **5**(90), 74091 (2015)
10. H. Firouzabadi, N. Iranpoor, M. Gholinejad, J. Hoseini, *Adv. Synth. Catal.* **353**, 125 (2011)
11. M. Hasan, G. Mustafa, J. Iqbal, M. Ashfaqa, N. Mahmood, *Toxicol. Res.* (2018). <https://doi.org/10.1039/C7TX00248C>
12. M. Hasan, Y. Yang, Y. JuXin Chu, Y. Wang, Y. Deng, N. Mahmood, Y. Hou, *Nano. Res.* **10**, 1912 (2017)
13. W.I. Gilbert, J. Turkevich, E.S. Wallis, *J. Org. Chem.* **3**, 611 (1938)
14. L.S. Glebov, G.A. Klinger, T.P. Popova, V.E. Shiryayeva, V.P. Ryzhikov, E.V. Marchevskaya, O.A. Lesik, S.M. Loktev, V.G. Beryezkin, *J. Mol. Catal.* **35**, 335 (1986)
15. Q. Liu, W. Ma, R. He, Z. Mu, *Catal. Today* **106**, 52 (2005)
16. A. Schple, U. Nieken, O. Shekhah, W. Ranke, R. Schlçgl, G. Kolios, *Phys. Chem. Chem. Phys.* **9**, 3619 (2007)
17. D. Guin, B. Baruwati, S.V. Manorama, *J. Mol. Catal. A Chem.* **242**, 26 (2005)
18. Y. Joseph, M. Wühn, A. Niklewski, W. Ranke, W. Weiss, C. Wöll, R. Schlögl, *Phys. Chem. Chem. Phys.* **2**, 5314 (2000)
19. H. Tang, X. Jian, B. Wu, S. Liu, Z. Jiang, X. Chen, W. Lv, W. He, W. Tian, Y. Wei, Y. Gao, T. Chen, G. Li, *Compos. Part B Eng.* **107**, 51 (2016)
20. E. Rafiee, M. Joshaghani, P.G.-S. Abadi, *J. Magn. Magn. Mater.* **408**, 107 (2016)
21. E. Rafiee, M. Kahrizi, M. Joshaghani, P.G.-S. Abadi, *Res. Chem. Intermed.* **42**, 5573 (2015)
22. S. Kang, Z. Jia, S. Shi, D.E. Nikles, J.W. Harrell, *Appl. Phys. Lett.* **86**, 062503 (2005)
23. M.A. Halcrow, *Spin-crossover materials: properties and applications* (Wiley, Hoboken, 2013)
24. A. Bousseksou, G. Molnár, L. Salmona, W. Nicolazzi, *Chem. Soc. Rev.* **40**(6), 3313 (2011)
25. A.Y. Yermakov, T.A. Feduschak, M.A. Uimin, A.A. Mysik, V.S. Gaviko, O.N. Chupakhin, A.B. Shishmakov, V.G. Kharchuk, L.A. Petrov, Y.A. Kotov, A.V. Vosmerikov, A.V. Korolyov, *Solid State Ion.* **172**(1), 317 (2004)

26. S. Kitashima, A. Kuroda, K. Hirosea, M. Sennaa, A.Y. Yermakovb, M.A. Uimin, J. Alloy. Compd. **434**, 646 (2007)
27. J. Sá, J. Szlachetko, M. Sikora, M. Kavčič, O.V. Safonova, M. Nachtegaal, *Nanoscale* **5**(18), 8462 (2013)
28. G. Yao, F. Wang, X. Wang, K. Gui, *Energy* **35**(5), 2295 (2010)
29. E. Rafiee, M. Joshaghani, P.G.-S. Abadi, *Arab. J. Chem.* (2015). <https://doi.org/10.1016/j.arabjc.2015.09.004>
30. E. Rafiee, M. Khodayari, *J. Mol. Catal. A Chem.* **398**, 336 (2015)
31. D.J. Ramo'n, M. Yus, *Chem. Rev.* **110**, 1611 (2010)
32. R.C.C. Costa, M.F.F. Lelis, L.C.A. Oliveira, J.D. Fabris, J.D. Ardisson, R.R.V.A. Rios, C.N. Silva, R.M. Lago, *J. Hazard. Mater.* **B129**, 171 (2006)
33. T. Zeng, W.W. Chen, C.M. Cirtiu, A. Moores, G. Song, C.J. Li, *Green Chem.* **12**, 570 (2010)
34. C. Cui, L. Gan, H.H. Li, S.H. Yu, M. Heggen, P. Strasser, *Nano Lett.* **12**, 5885 (2012)
35. M. Crespo-Quesada, A. Yarulin, M. Jin, Y. Xia, L. Kiwi Minsker, *J. Am. Chem. Soc.* **133**, 12787 (2011)
36. M. Jin, H. Zhang, Z. Xie, Y. Xia, *Angew. Chem. Int. Ed.* **50**, 7850 (2011)
37. A. Mohanty, N. Garg, R. Jin, *Angew. Chem. Int. Ed.* **49**, 4962 (2010)
38. X. Jian, S. Liu, Y. Gao, W. Zhang, W. He, A. Mahmood, C.M. Subramaniam, X. Wang, N. Mahmood, S. Dou, *Appl. Mater. Interfaces* **9**(22), 18872 (2017)
39. G. Sun, Z. Wang, *Tetrahedron Lett.* **49**(33), 4929 (2008)
40. M.M. Mojtahedi, M.S. Abaee, T. Alishiri, *Tetrahedron Lett.* **50**, 2322 (2009)
41. R.A. Crane, M. Dickinson, I.C. Popescu, T.B. Scott, *Water Res.* **45**, 2931 (2011)
42. K.I. Fujita, Z. Li, N. Ozekib, R. Yamaguchi, *Tetrahedron Lett.* **44**(13), 2687 (2003)
43. I. Geukens, F. Vermoortele, M. Meledina, S. Turner, G. Van-Tendeloo, D.E. De-Vos, *Appl. Catal. A Gen.* **469**, 373 (2014)
44. H. Yang, R. Mao, C. Luo, C. Lu, G. Cheng, *Tetrahedron* **70**(46), 8829 (2014)
45. X.H. Lu, Y.W. Sun, X.L. Wei, C. Peng, D. Zhou, Q.H. Xia, *Catal. Commun.* **55**, 78 (2014)
46. R. Kawahara, K. Fujita, R. Yamaguchi, *Adv. Synth. Catal.* **353**(7), 1161 (2011)
47. C. Gonzalez-Arellano, K. Yoshida, R. Luque, P.L. Gai, *Green Chem.* **12**(7), 1281 (2010)
48. K.I. Shimizu, N. Imaiida, K. Kon, S.M.A. Hakim-Siddiki, A. Satsuma, *ACS. Catal.* **3**(5), 998 (2013)
49. Q. Li, S. Fan, Q. Sun, H. Tian, X. Yu, Q. Xu, *Org. Biomol. Chem.* **10**(15), 2966 (2012)
50. M.M. Reddy, M.A. Kumar, P. Swamy, M. Naresh, K. Srujana, L. Satyanarayana, A. Venugopal, N. Narender, *Green Chem.* **15**(12), 3474 (2013)
51. H. Liu, G.K. Chuah, S. Jaenicke, *J. Catal.* **292**, 130 (2012)
52. A.M. Rasero-Almansa, A. Corma, M. Iglesias, F. Sanchez, *Chem. Cat. Chem.* **6**(6), 1794 (2014)
53. R. Ramachandran, G. Prakash, S. Selvamurugan, P. Viswanathamurthi, J.G. Malecki, V. Ramkumar, *Dalton Trans.* **43**(21), 7889 (2014)
54. R. Martínez, D.J. Ramón, M. Yus, *Org. Biomol. Chem.* **7**(10), 2176 (2009)
55. Y. Zhang, X. Qi, X. Cui, F. Shi, Y. Deng, *Tetrahedron Lett.* **52**(12), 1334 (2011)
56. K. Fujita, Y. Enoki, R. Yamaguchi, *Tetrahedron* **64**(8), 1943 (2008)
57. T. Yan, B.L. Feringa, K. Barta, *Nat. Commun.* **5**, 5602 (2014)
58. M.M. Reddy, M.A. Kumar, P. Swamy, M. Naresh, K. Srujana, L. Satyanarayana, A. Venugopal, N. Narender, *Green Chem.* **15**, 3474 (2013)
59. R. Ramachandran, G. Prakash, S. Selvamurugan, P. Viswanathamurthi, J.G. Malecki, V. Ramkumar, *Dalton Trans.* **43**, 7889 (2014)
60. S. Roy, S. Podder, J. Choudhury, *J. Chem. Sci.* **120**(5), 429 (2008)
61. T. Tsuchimoto, K. Tobita, T. Hiyama, S. Fukuzawa, *J. Org. Chem.* **62**(20), 6997 (1997)
62. B.Q. Wang, S.K. Xiang, Z.P. Sun, B.T. Guan, P. Hu, K.Q. Zhao, Z.J. Shi, *Tetrahedron Lett.* **49**(27), 4310 (2008)
63. H.B. Sun, *Tetrahedron* **63**(41), 10185 (2007)
64. B. Jäger, A. Wermann, P. Scholza, M. Müllerb, U. Reislöhner, A. Stollea, B. Ondruschka, *Appl. Catal. A: Gen.* **443**, 87 (2012)
65. Y. Sato, *Tetrahedron* **68**(35), 7077 (2012)
66. D.F. Bagster, *Int. J. Miner. Process.* **20**, 1 (1987)
67. A. Junod, M. Roulin, B. Revaz, A. Mirmelstein, J.Y. Genoud, E. Walker, A. Erb, *Phys. C* **282–287**, 1399 (1997)